



Synthesis, molecular docking and biological evaluation of 1,3,4-oxadiazole derivatives as potential immunosuppressive agents

Ru Yan, Zhi-Ming Zhang, Xian-Ying Fang, Yang Hu, Hai-Liang Zhu*

State Key Laboratory of Pharmaceutical Biotechnology, Nanjing University, Nanjing 210093, People's Republic of China

ARTICLE INFO

Article history:

Received 20 December 2011

Revised 11 January 2012

Accepted 12 January 2012

Available online 25 January 2012

Keywords:

Oxadiazoles

Immunosuppressive activity

Molecular docking

PI3K γ

ABSTRACT

A series of novel 1,3,4-oxadiazole derivatives (**5a–5s**) have been designed, synthesized and evaluated for their immunosuppressive activity. Most of these synthesized compounds were proved to have potent immunosuppressive activity and low toxicity. Among them, compounds (**5m–5r**) showed the most potent biological activity against lymph node cells. The results of flow cytometry (FCM) and western blotting demonstrated that compound **5q** induce cell apoptosis by the inhibition of PI3 K/AKT pathway. Molecular docking was performed to position compound **5q** into PI3K γ binding site in order to explore the potential target.

© 2012 Published by Elsevier Ltd.

1. Introduction

Immunosuppressant is a kind of drugs that can reduce the body's immune reaction by inhibiting the immune cells proliferation, that is commonly used to transplant rejection and the treatment of autoimmune diseases such as systemic lupus erythematosus, rheumatoid arthritis and psoriasis.^{1–3} Phosphoinositide 3-kinases (PI3 Ks), key components of the PI3 K/AKT pathway which plays essential roles in various cellular activities, are lipid kinases that phosphorylate the 3-hydroxyl group of phosphoinositides.⁴ PI3 Ks are grouped into three classes (I, II, and III) according to their structure preference and substrate specificity, class I PI3Ks are separated into two subfamilies (IA and IB) depending on the receptors to which they couple.^{5,6} Among these isoforms, PI3K γ (the only isoform of class IB) plays a pivotal role in inflammation, and it is involved in allergy, development of chronic inflammation, autoimmune diseases.^{7,8} Therefore, there is important significance to discover a kind of drug that can influence PI3K γ .

Compounds containing a 1,4-benzodioxan template (Fig. 1) with acetic acid substituent on C6 or C2 (A and B) have anti-inflammatory activity.^{9,10} However, compound B have a better activity, it can be used as a nonsteroidal anti-inflammatory drug (NSAID).⁹ A series of derivatives containing a 1,4-benzodioxan template were designed and synthesized by Harrak, and among them, compounds C and D (Fig. 1) showed good anti-inflammatory activity.^{11,12}

Oxadiazoles are an important class of heterocyclic compounds, which have been reported to have many various activities,¹³ such

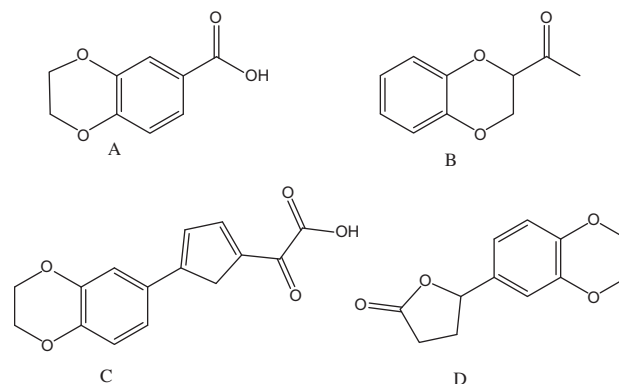


Figure 1. The structure of compounds A–D.

as hypoglycemic,¹⁴ anti-viral,¹⁵ anti-cancer,¹⁶ anti-bactericidal¹⁷ effects. In particular, a few substituted 1,3,4-oxadiazoles have been found to exhibit immunosuppressive activities.^{18–21} Therefore, oxadiazole derivatives have raised considerable attention to medicinal research, and a large number of investigations on their synthesis and biological activities have been reported during the last 10 years.^{22–25}

A series of novel oxadiazoles compounds containing a 1,4-benzodioxan template were firstly synthesized and anti-inflammatory activities were detected. Among them, the compounds **5m–5r** displayed potent immunosuppressive activity by inhibiting ConA co-stimulated lymph node cells proliferation and had low toxicity. Preliminary study on the immune mechanism of the compounds

* Corresponding author. Tel.: +86 25 8359 2572; fax: +86 25 8359 2672.

E-mail address: zhuhl@nju.edu.cn (H.-L. Zhu).

found that compounds induced cell apoptosis by the inhibition of PI3 K/AKT pathway. From the results, we can conclude that some of the synthesized compounds are potent immunosuppressant.

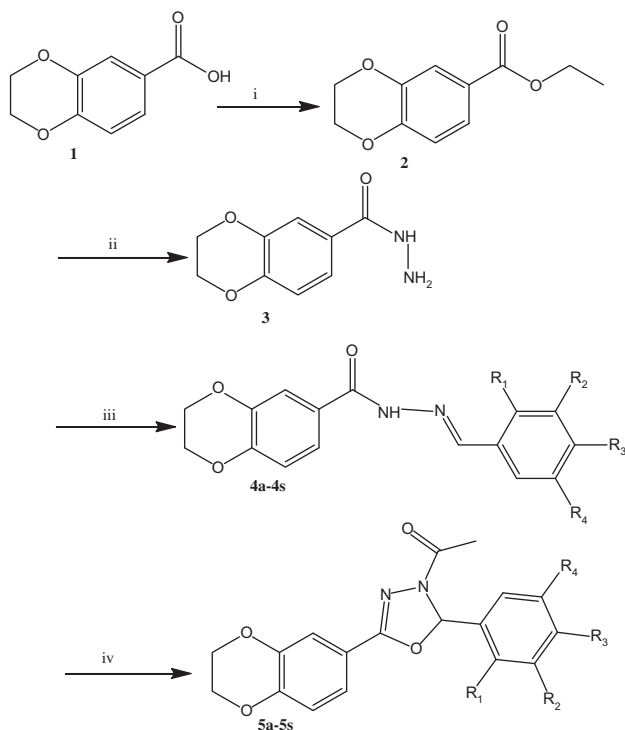
2. Results and discussion

2.1. Chemistry

Nineteen 1,3,4-oxadiazole derivatives (**5a–5s**) were firstly synthesized to screen for the anti-inflammatory activity. The synthetic route was based on the following sequence of reactions,^{26–28} as shown in Scheme 1. As an example, the reaction of 2,3-dihydrobenzo[b][1,4]dioxine-6-carboxylic acid with concentrated H_2SO_4 was refluxed in ethanol for overnight to produce the corresponding ester. Secondly, a mixture of the ester and hydrazine hydrate in ethanol was refluxed for overnight, by which the corresponding hydrazide was formed. Thirdly, the hydrazone products were synthesized by refluxing the mixture of hydrazide and the different substituted benzaldehyde in ethanol for 5 h. The hydrazone and glacial acetic acid in acetic anhydride were refluxed for 1 h, after which the mixture was poured into ice water and oxadiazoline analogs were collected. When needed, oxadiazoline analogs were purified by recrystallization in aqueous methanol. All structure of the synthetic compounds were shown in Table 1.

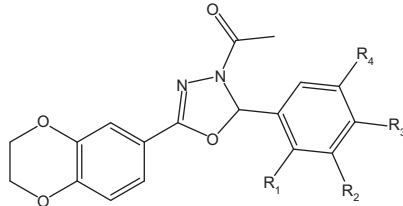
2.2. Crystal structure of compound 5r

Among these compounds, a crystal structure of compound **5r** was determined by X-ray diffraction analysis. The crystal data are presented in Table 2 and Fig. 2 give perspective views of **5r** with the atomic labeling system.



Scheme 1. General synthesis of compounds **5a–5s**. Reagents and conditions: (i) ethanol, concentrated sulfuric acid; reflux; (ii) hydrazine hydrate, ethanol; reflux; (iii) substituted benzaldehyde, ethanol, reflux; (iv) acetic anhydride, glacial acetic acid, reflux.

Table 1
Structure of oxadiazole derivatives



Compound	R ₁	R ₂	R ₃	R ₄
5a	H	H	H	H
5b	Cl	H	H	H
5c	H	H	NO ₂	H
5d	H	H	OMe	H
5e	H	H	Me	H
5f	H	OMe	H	H
5g	F	H	H	H
5h	H	Br	H	H
5i	H	H	OCH ₂ Ph	H
5j	Cl	H	Cl	H
5k	H	F	H	H
5l	H	H	F	H
5m	H	H	OCOCH ₃	H
5n	OCOCH ₃	H	H	H
5o	OCOCH ₃	H	H	Cl
5p	OCOCH ₃	H	H	Br
5q	OCOCH ₃	Cl	H	Cl
5r	OCOCH ₃	Br	H	Br

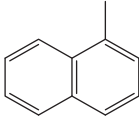
Compound	R ₁	R ₂	R ₃	R ₄
5s			H	H

Table 2
Crystal data for compound **5r**

Crystal parameters	Compound 5r
Formula	C ₂₀ H ₁₆ Br ₂ N ₂ O ₆
Crystal size (mm)	0.2 × 0.2 × 0.1
MW (g mol ⁻¹)	537.94
Crystal system	Monoclinic
α (°)	90.00
β (°)	111.259(6)
γ (°)	90.00
a (Å)	12.094(8)
b (Å)	12.410(8)
c (Å)	14.889(9)
V (Å ³)	2082(2)
Z	4
θ limits (°)	2.20 ≤ θ ≤ 29.03
hkl limits	−16 ≤ h ≤ 15, −16 ≤ k ≤ 16, −18 ≤ l ≤ 20
F(000)	1482
Data/restraints/parameters	5200/0/271
Absorption coefficient (mm ⁻¹)	12.565
Reflections collected	17597
Independent reflections	5200 [R _{int} = 0.1082]
R ₁ /wR ₂ [I > 2σ(I)]	0.0759/0.1457
R ₁ /wR ₂ (all data)	0.1786/0.1877
GOF	1.024

2.3. Immunosuppressive activity

2.3.1. Cytotoxicity test

Generally speaking, the inhibitory activity of the compounds is due to cell apoptosis or toxic effect, so we firstly performed cytotoxicity test before detecting biological activity. The oxadiazole compounds were detected for their cytotoxicity on lymph node cells with cyclosporin A (CsA) as the positive control. The

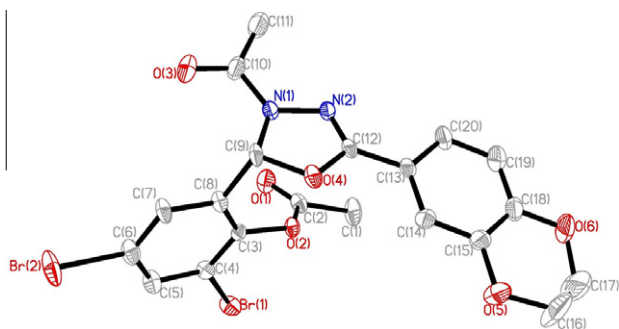


Figure 2. Crystal structure diagrams of compound **5r**.

Table 3

Cytotoxicity assay and inhibitory activity of the compounds on lymph node cells

Compound	CC ₅₀ ± SD (μM)	IC ₅₀ ± SD (μM)	SI
5a	209.99 ± 25.04	36.06 ± 0.39	5.82
5b	343.16 ± 36.30	52.35 ± 5.64	6.56
5c	363.72 ± 21.21	>100	<3.63
5d	412.36 ± 34.13	95.36 ± 6.78	4.27
5e	258.59 ± 18.16	17.06 ± 0.60	15.15
5f	293.17 ± 24.78	72.08 ± 3.87	4.07
5g	304.19 ± 27.35	33.90 ± 1.36	8.97
5h	275.68 ± 18.14	9.08 ± 0.31	30.36
5i	248.25 ± 21.63	49.83 ± 4.32	4.98
5j	268.74 ± 22.86	30.98 ± 6.32	8.67
5k	210.51 ± 19.53	52.42 ± 5.43	4.02
5l	298.08 ± 18.35	82.83 ± 7.56	3.59
5m	491.43 ± 37.86	7.46 ± 0.37	65.88
5n	288.37 ± 21.52	2.16 ± 0.12	133.51
5o	225.63 ± 37.34	1.22 ± 0.09	184.94
5p	261.89 ± 27.45	1.43 ± 0.13	183.14
5q	363.36 ± 28.34	1.83 ± 0.18	198.56
5r	332.28 ± 25.68	2.03 ± 0.23	163.68
5s	323.71 ± 23.67	>100	<3.23
CsA	13.78 ± 1.87	0.07 ± 0.01	196.86

pharmacological results of these compounds were summarized in Table 3. What we can see from the data is that most of the compounds were low toxic.

2.3.2. Inhibitory activity on lymph node cells

All the compounds were tested in vitro for the inhibition activity on ConA stimulated lymph node cells. The results were summarized in Table 3. The table showed that most of the synthesized compounds showed potent inhibitory activity with the IC₅₀ value at low micromolar.

Structure–activity relationships (SARs) were inferred from Table 3. In general, compounds with electronic-withdrawing substituents (halogen or acetoxy) on the benzene ring showed more potent inhibitory activities than compounds only contained electronic-donating substituents (methyl or methoxy) on the benzene ring. Exceptionally compounds (**5m–5r**) with acetoxy on the benzene ring exhibited higher immunosuppressive activity compared with other compounds. Among the compounds of acetoxy substituents, the activities of Cl substituent is a little higher activity than that of Br substituent (**5o** > **5p**, **5q** > **5r**). The position of substituents on benzene ring also influenced the activities. For example, the order of the activities is that substituent at the *ortho* (**5g**) position > substituent at the *meta* (**5k**) position > substituent at the *para* (**5l**) position.

Among them, compound **5o** displayed the best immunosuppression activity, as it has the lowest IC₅₀ (IC₅₀ = 1.22 μM). However, the cytotoxicity and SI (SI = 198.56) of the compound **5q** have absolute advantage compared to others. Our goal is to explore

the potential drug which has high activity and low toxicity. Considering the two factors, compound **5q** may be a potential anti-inflammatory drug with high efficacy (IC₅₀ = 1.83 μM) and low toxicity (CC₅₀ = 363.36 μM).

2.3.3. PI3Kγ enzymatic activity

The PI3Kγ inhibitory potency of oxadiazole derivatives was examined and the results were presented in Table 4. The tested compounds showed potent PI3Kγ inhibitory. The results of PI3Kγ inhibitory activity of the tested compounds were corresponding to the structure relationships (SARs) of their inhibitory effects on lymph node cells. The results suggested that inhibitory activity on lymph node cells of the compounds may by inhibiting PI3Kγ enzymatic activity.

2.3.4. Apoptosis assay

In order to study the preliminary anti-inflammatory mechanism of the compounds, we performed flow cytometry (FCM) (Fig. 3). As shown in Figure 3, lymph node cells were treated with 0, 3, 10 and 30 μM of compounds **5n** and **5q** for 24 h. The compounds can increase the percentage of apoptosis in a dose-independent manner. The results indicated that compounds **5n** and **5q** can induce apoptosis of ConA stimulated lymph node cells, exceptionally compound **5q** obviously induced apoptosis.

2.3.5. Western blotting

To determine whether target compounds suppress activation of AKT (a key downstream effector of PI3K and important node in the PI3K/AKT/mTOR signaling pathway) and Caspase 3 (an important enzyme in apoptosis), selected compound **5q** were tested for its suppression on p-AKT and Cleaved Caspase 3. As shown in Figure 4, p-AKT (pS473) was dose-dependent lower regulated upon **5q** treated for 24 h. The activity of Cleaved Caspase 3 was dose-dependent up-regulated upon **5q** treated. It can be conferred from the result that the apoptosis induced by **5q** may be mediated by the inhibition of PI3K/AKT pathway.

2.4. Binding model of compounds 5q into PI3Kγ structure

To gain better understanding on the potency of the synthesized compounds and guide further structure–activity relationships (SARs) studies. The molecular docking was performed by potent inhibitor **5q** into binding site of PI3Kγ. All docking runs were applied Discovery Studio3.1 (DS. 3.1). The binding modes of compound **5q** and PI3Kγ were depicted in Figures 5 and 6. In the binding mode, compound **5q** is nicely bound to the PI3Kγ via two hydrogen bonds and Pi-sigma. Cl atom on the benzene ring and amino hydrogen of LYS 890 form hydrogen bond (H–Cl...H: 2.47 Å, 158.4°), the oxygen atom of the benzene group also form hydrogen bond (H–O...H: 2.46 Å, 157.3°) with hydrogen atom of VAL 882. Pi-sigma (2.92 Å) is formed by SER 806 with benzene ring. The results of molecular docking and western blotting show that compound **5q** influence the expression of downstream protein by bonding to PI3Kγ. These results, along with the date of inhibitory

Table 4

PI3Kγ inhibitory activity of the selected compounds

Compound	PI3Kγ IC ₅₀ (μM)
5n	2.06
5o	0.98
5p	1.31
5q	1.75
5r	1.98
LY294002 ^a	7.26

^a Reported value, Ref. 29.

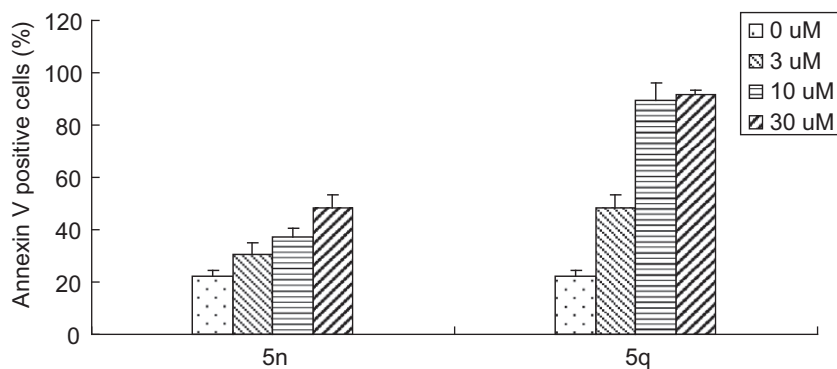


Figure 3. Lymph node cells were stimulated with ConA for 24 h, and then various concentrations of compounds **5n** and **5q** were added to incubate for 24 h. Cells were stained by Annexin V-FITC and datas were analyzed by flow cytometry (FCM).

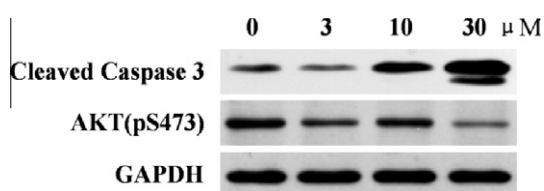


Figure 4. Western blotting was performed to detect the effect of compound **5q** on p-AKT (pS473) and Cleaved Caspase3.

3. Conclusions

A series of novel oxadiazole compounds have been designed and firstly synthesized and their biological activities were also evaluated as potent anti-inflammatory activity. Among them, compound **5q** demonstrated the potent inhibitory activity ($IC_{50} = 1.83 \mu M$, $SI = 198.56$) compared to positive control ($IC_{50} = 0.07 \mu M$, $SI = 196.86$). The results of flow cytometry (FCM) and western blotting demonstrated that compound **5q** induced cell apoptosis by the inhibition of PI3K/AKT pathway. Molecular docking showed that compound **5q** bound to PI3K γ by two hydrogen bonds and a Pi-sigma. This study showed that compound **5q** may be a potential anti-inflammatory drug.

activity assay indicated that compound **5q** would be a kind of potential inhibitor.

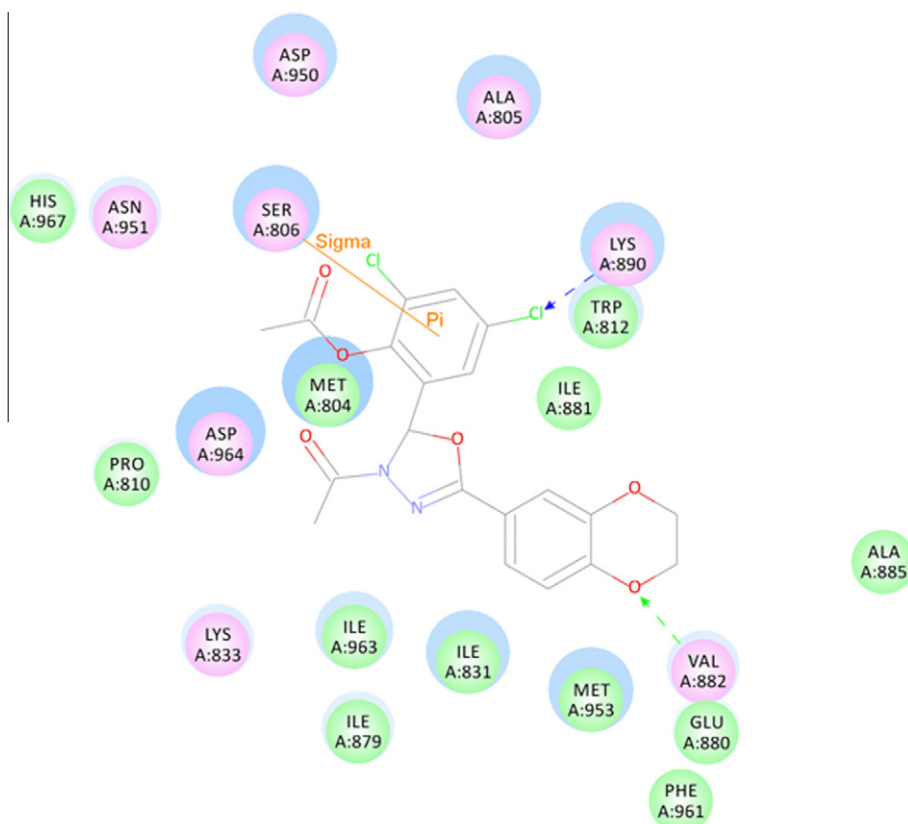


Figure 5. The molecular docking of compound **5q** into PI3K. Compound **5q** is nicely bound to the PI3K via two hydrogen bonds ($H-Cl \cdots H$: 2.47 Å, 158.4°, $H-O \cdots H$: 2.46 Å, 157.3°) and Pi-sigma (2.92 Å).

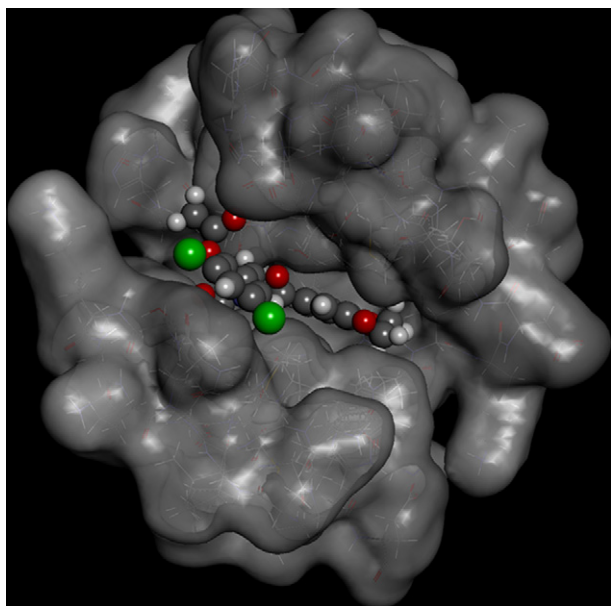


Figure 6. 3D model of the interaction between compound **5q** and PI3K bonding site. The protein is represented by molecular surface. Compound **5q** is depicted by balls.

4. Experimental section

4.1. Methods of synthesis

Melting points (uncorrected) were determined on an XT4 MP apparatus (Taikang Corp., Beijing, China). ESI mass spectra were obtained on a Mariner System 5304 mass spectrometer, and ^1H NMR spectra were recorded on a Bruker PX500 or DPX300 spectrometer at 25 °C with TMS and solvent signals allotted as internal standards. Chemical shifts were reported in ppm (δ). Elemental analyses were performed on a CHN-O-Rapid instrument and were within 0.4% of the theoretical values.

4.1.1. Synthesis of 2,3-dihydrobenzo[*b*][1,4]dioxine-6-carboxylate (**2**)

The 2,3-dihydrobenzo[*b*][1,4]dioxine-6-carboxylic acid (9.0 g, 50 mmol) was dissolved in anhydrous ethanol (50 mL) containing concentrated H_2SO_4 (5 mL), which were refluxed overnight. The solvent was evaporated until no longer liquid outflow. Water (20 mL) was added, extracting by adding respectively 40, 30 and 20 mL ethyl acetate. The organic phases were sequentially washed with saturated NaHCO_3 , brine, and dried over MgSO_4 . The solvent was removed under reduced pressure to yield compound **2**.

4.1.2. Synthesis of 2,3-dihydrobenzo[*b*][1,4]dioxine-6-carbohydrazide (**3**)

To compound **2** (0.05 mol) dissolved in anhydrous ethanol (35 mL), hydrazine hydrate (15 mL) was added and the mixture was refluxed for 24 h. The reaction mixture was evaporated and until no longer liquid outflow. Then water was added and compound **3** was precipitated.

4.1.3. Synthesis of *N*'-benzylidenebenzohydrazide (**4**)

To a stirred solution of hydrazide (1 mmol) and appropriate benzaldehyde in ethanol (25 mL), water (5 mL) was added followed by dropwise addition of glacial acetic acid (0.2 mL). The mixture was refluxed for 5 h, after which the solution was poured into ice water. The mixture was stirred until precipitate formed, which was collected using suction filtration and dried, followed

by recrystallization in anhydrous ethanol, giving compound **4** as a white solid.

4.1.4. Synthesis of 1-(5-(2,3-dihydrobenzo[*b*][1,4]dioxin-6-yl)-1,3,4-oxadiazol-3(2*H*)-yl)ethanone (**5**)

Compound **4** (0.001 mol) and glacial acetic acid (2 mL) were added in Ac_2O (5 mL), and the resulting solution was heated to reflux for 1 h. The reaction mixture was poured into ice water, which was collected using suction filtration and dried, followed by recrystallization in anhydrous ethanol, followed by drying to yield **5a–5s**.

4.1.4.1. 1-(5-(2,3-Dihydrobenzo[*b*][1,4]dioxin-6-yl)-2-phenyl-1,3,4-oxadiazol-3(2*H*)-yl)ethanone (5a**).** White solid, yield 73%, mp: 129–130 °C. ^1H NMR (CDCl_3 , 300 MHz): 2.33 (s, 3H), 4.26–4.32 (m, 4H), 6.89–6.92 (m, 1H), 7.05 (s, 1H), 7.37–7.40 (m, 5H), 7.42–7.48 (m, 2H). MS (ESI): 325.1 ($\text{C}_{18}\text{H}_{17}\text{N}_2\text{O}_4$, $[\text{M}+\text{H}]^+$). Anal. Calcd for $\text{C}_{18}\text{H}_{16}\text{N}_2\text{O}_4$: C, 66.66; H, 4.97; N, 8.64; O, 19.73. Found: C, 66.68; H, 4.99; N, 8.63.

4.1.4.2. 1-(2-(2-Chlorophenyl)-5-(2,3-dihydrobenzo[*b*][1,4]dioxin-6-yl)-1,3,4-oxadiazol-3(2*H*)-yl)ethanone (5b**).** White solid, yield 69%, mp: 171–172 °C. ^1H NMR (300 MHz, $\text{DMSO}-d_6$) δ : 2.26 (s, 3H), 4.29–4.30 (m, 4H), 6.98 (d, $J = 8.4$ Hz, 1H), 7.22 (d, $J = 2.0$ Hz, 1H), 7.28–7.31 (m, 2H), 7.41–7.51 (m, 3H), 7.56 (d, $J = 7.9$ Hz, 1H). MS (ESI): 359.8 ($\text{C}_{18}\text{H}_{16}\text{ClN}_2\text{O}_4$, $[\text{M}+\text{H}]^+$). Anal. Calcd for $\text{C}_{18}\text{H}_{15}\text{ClN}_2\text{O}_4$: C, 60.26; H, 4.21; N, 7.81. Found: C, 60.24; H, 4.21; N, 7.83.

4.1.4.3. 1-(5-(2,3-Dihydrobenzo[*b*][1,4]dioxin-6-yl)-2-(4-nitrophenyl)-1,3,4-oxadiazol-3(2*H*)-yl)ethanone (5c**).** Yellow solid, Yield 60%; mp: 151–152 °C. ^1H NMR ($\text{DMSO}-d_6$, 300 MHz): 2.25 (s, 3H), 4.28–4.31 (m, 4H), 7.01 (d, $J = 8.40$ Hz, 1H), 7.27–7.31 (m, 2H), 7.32–7.36 (m, 1H), 7.76 (d, $J = 8.79$ Hz, 2H), 8.29 (d, $J = 8.61$ Hz, 2H). MS (ESI): 370.10 ($\text{C}_{18}\text{H}_{16}\text{N}_3\text{O}_6$, $[\text{M}+\text{H}]^+$). Anal. Calcd for $\text{C}_{18}\text{H}_{15}\text{N}_3\text{O}_6$: C, 58.54; H, 4.09; N, 11.38; O, 25.99. Found: C, 58.53; H, 4.09; N, 11.40.

4.1.4.4. 1-(5-(2,3-Dihydrobenzo[*b*][1,4]dioxin-6-yl)-2-(4-methoxyphenyl)-1,3,4-oxadiazol-3(2*H*)-yl)ethanone (5d**).** White solid, yield 70%, mp: 153–154 °C. ^1H NMR (300 MHz, $\text{DMSO}-d_6$) δ : 2.22 (s, 3H), 3.76 (s, 3H), 4.29–4.30 (m, 4H), 6.96–7.00 (m, 3H), 7.09 (s, 1H), 7.23 (d, $J = 2.0$ Hz, 1H), 7.29–7.33 (m, 1H), 7.36 (d, $J = 8.6$ Hz, 2H). MS (ESI): 355.4 ($\text{C}_{19}\text{H}_{19}\text{N}_2\text{O}_5$, $[\text{M}+\text{H}]^+$). Anal. Calcd for $\text{C}_{19}\text{H}_{18}\text{N}_2\text{O}_5$: C, 64.40; H, 5.12; N, 7.91. Found: C, 64.42; H, 5.10; N, 7.90.

4.1.4.5. 1-(5-(2,3-Dihydrobenzo[*b*][1,4]dioxin-6-yl)-2-(*p*-tolyl)-1,3,4-oxadiazol-3(2*H*)-yl)ethanone (5e**).** White solid, yield 62%, mp: 115–116 °C. ^1H NMR (300 MHz, $\text{DMSO}-d_6$) δ : 2.22 (s, 3H), 2.31 (s, 3H), 4.28–4.30 (m, 4H), 6.99 (d, $J = 8.4$ Hz, 1H), 7.10 (s, 1H), 7.22–7.24 (m, 3H), 7.30–7.33 (m, 3H). MS (ESI): 339.4 ($\text{C}_{19}\text{H}_{19}\text{N}_2\text{O}_4$, $[\text{M}+\text{H}]^+$). Anal. Calcd for $\text{C}_{19}\text{H}_{18}\text{N}_2\text{O}_4$: C, 67.44; H, 5.36; N, 8.28. Found: C, 67.40; H, 5.35; N, 8.30.

4.1.4.6. 1-(5-(2,3-Dihydrobenzo[*b*][1,4]dioxin-6-yl)-2-(3-methoxyphenyl)-1,3,4-oxadiazol-3(2*H*)-yl)ethanone (5f**).** White solid, yield 64%, mp: 124–125 °C. ^1H NMR (300 MHz, $\text{DMSO}-d_6$) δ : 2.22 (s, 3H), 3.74 (s, 3H), 4.28–4.29 (m, 4H), 6.96–6.99 (m, 4H), 7.09 (s, 1H), 7.23 (d, $J = 2.0$ Hz, 1H), 7.29–7.33 (m, 2H). MS (ESI): 355.4 ($\text{C}_{19}\text{H}_{19}\text{N}_2\text{O}_5$, $[\text{M}+\text{H}]^+$). Anal. Calcd for $\text{C}_{19}\text{H}_{18}\text{N}_2\text{O}_5$: C, 64.40; H, 5.12; N, 7.91. Found: C, 64.45; H, 5.10; N, 7.92.

4.1.4.7. 1-(5-(2,3-Dihydrobenzo[*b*][1,4]dioxin-6-yl)-2-(2-fluorophenyl)-1,3,4-oxadiazol-3(2*H*)-yl)ethanone (5g**).** White solid, yield 76%, mp: 127–128 °C. ^1H NMR (300 MHz, CDCl_3) δ : 2.35 (s, 3H), 4.26–4.33 (m, 4H), 6.88–6.91 (m, 1H), 7.07–7.18 (m, 2H),

7.23 (s, 1H), 7.34–7.40 (m, 4H). MS (ESI): 343.3 ($C_{18}H_{16}FN_2O_4$, $[M+H]^+$). Anal. Calcd for $C_{18}H_{15}FN_2O_4$: C, 63.15; H, 4.42; F, 5.55; N, 8.18. Found: C, 63.11; H, 4.43; N, 5.57.

4.1.4.8. 1-(2-(3-Bromophenyl)-5-(2,3-dihydrobenzo[b][1,4]dioxin-6-yl)-1,3,4-oxadiazol-3(2H)-yl)ethanone (5h). White solid, yield 64%, mp: 142–143 °C. 1H NMR (300 MHz, $CDCl_3$) δ : 2.34 (s, 3H), 4.28–4.32 (m, 4H), 6.90–6.93 (m, 1H), 7.00 (s, 1H), 7.24–7.29 (m, 1H), 7.38–7.44 (m, 3H), 7.51 (d, $J = 7.9$ Hz, 1H), 7.59 (d, $J = 1.7$ Hz, 1H). MS (ESI): 404.2 ($C_{18}H_{16}BrN_2O_4$, $[M+H]^+$). Anal. Calcd for $C_{18}H_{15}BrN_2O_4$: C, 53.62; H, 3.75; N, 6.95. Found: C, 53.66; H, 3.74; N, 6.93.

4.1.4.9. 1-(2-(4-(Benzyloxy)phenyl)-5-(2,3-dihydrobenzo[b][1,4]dioxin-6-yl)-1,3,4-oxadiazol-3(2H)-yl)ethanone (5i). White solid, yield 69%, mp: 131–132 °C. 1H NMR (300 MHz, $DMSO-d_6$) δ : 2.22 (s, 3H), 4.29–4.30 (m, 4H), 5.12 (s, 2H), 6.99 (d, $J = 8.4$ Hz, 1H), 7.03–7.08 (t, $J = 7.4$ Hz, 3H), 7.23 (d, $J = 2.0$ Hz, 1H), 7.29–7.45 (m, 8H). MS (ESI): 540.2 ($C_{25}H_{23}N_2O_5$, $[M+H]^+$). Anal. Calcd for $C_{25}H_{22}N_2O_5$: C, 69.76; H, 5.15; N, 6.51. Found: C, 69.73; H, 5.12; N, 5.54.

4.1.4.10. 1-(2-(2,4-Dichlorophenyl)-5-(2,3-dihydrobenzo[b][1,4]dioxin-6-yl)-1,3,4-oxadiazol-3(2H)-yl)ethanone (5j). White solid, yield 65%, mp: 136–138 °C. 1H NMR (300 MHz, $DMSO-d_6$) δ : 2.25 (s, 3H), 4.29–4.30 (m, 4H), 6.98 (d, $J = 8.4$ Hz, 1H), 7.22 (d, $J = 2.1$ Hz, 1H), 7.28–7.31 (m, 2H), 7.46–7.53 (m, 2H), 7.75 (d, $J = 1.62$ Hz, 1H). MS (ESI): 394.2 ($C_{18}H_{15}Cl_2N_2O_4$, $[M+H]^+$). Anal. Calcd for $C_{18}H_{14}Cl_2N_2O_4$: C, 54.98; H, 3.59; Cl, 18.03; N, 7.12. Found: C, 54.95; H, 3.61; N, 7.10.

4.1.4.11. 1-(5-(2,3-Dihydrobenzo[b][1,4]dioxin-6-yl)-2-(3-fluorophenyl)-1,3,4-oxadiazol-3(2H)-yl)ethanone (5k). White solid, yield 69%, mp: 129–130 °C. 1H NMR (300 MHz, $DMSO-d_6$) δ : 2.24 (s, 3H), 4.28–4.31 (m, 4H), 7.01 (d, $J = 8.6$ Hz, 1H), 7.17 (s, 1H), 7.25–7.35 (m, 5H), 7.46–7.53 (m, 1H). MS (ESI): 343.3 ($C_{18}H_{16}FN_2O_4$, $[M+H]^+$). Anal. Calcd for $C_{18}H_{15}FN_2O_4$: C, 63.15; H, 4.42; F, 5.55; N, 8.18. Found: C, 63.12; H, 4.40; N, 8.19.

4.1.4.12. 1-(5-(2,3-Dihydrobenzo[b][1,4]dioxin-6-yl)-2-(4-fluorophenyl)-1,3,4-oxadiazol-3(2H)-yl)ethanone (5l). White solid, yield 69%, mp: 123–124 °C. 1H NMR (300 MHz, $CDCl_3$) δ : 2.32 (s, 3H), 4.27–4.32 (m, 4H), 6.89–6.92 (m, 1H), 7.03–7.09 (m, 3H), 7.37–7.40 (m, 2H), 7.43–7.48 (m, 2H). MS (ESI): 343.3 ($C_{18}H_{16}FN_2O_4$, $[M+H]^+$). Anal. Calcd for $C_{18}H_{15}FN_2O_4$: C, 63.15; H, 4.42; N, 8.18. Found: C, 63.18; H, 4.40; N, 8.15.

4.1.4.13. 4-(3-Acetyl-5-(2,3-dihydrobenzo[b][1,4]dioxin-6-yl)-2,3-dihydro-1,3,4-oxadiazol-2-yl)phenyl acetate (5m). White solid, yield 66%, mp: 143–144 °C. 1H NMR (300 MHz, $DMSO-d_6$) δ : 2.24–2.27 (m, 6H), 4.29–4.31 (m, 4H), 6.99 (d, $J = 8.6$ Hz, 1H), 7.17–7.20 (t, $J = 5.78$ Hz, 3H), 7.26 (d, $J = 2.0$ Hz, 1H), 7.33 (dd, $J = 8.4$ Hz, 1H), 7.49 (d, $J = 8.6$ Hz, 2H). MS (ESI): 383.4 ($C_{20}H_{19}N_2O_6$, $[M+H]^+$). Anal. Calcd for $C_{20}H_{18}N_2O_6$: C, 62.82; H, 4.74; N, 7.33. Found: C, 62.85; H, 4.72; N, 7.32.

4.1.4.14. 2-(3-Acetyl-5-(2,3-dihydrobenzo[b][1,4]dioxin-6-yl)-2,3-dihydro-1,3,4-oxadiazol-2-yl)phenyl acetate (5n). White solid, yield 60%, mp: 158–160 °C. 1H NMR (300 MHz, $DMSO-d_6$) δ : 2.12–2.18 (m, 6H), 4.26–4.29 (m, 4H), 6.98 (d, $J = 8.6$ Hz, 1H), 7.13–7.19 (m, 3H), 7.26–7.32 (m, 2H), 7.46–7.51 (m, 2H). MS (ESI): 383.4 ($C_{20}H_{19}N_2O_6$, $[M+H]^+$). Anal. Calcd for $C_{20}H_{18}N_2O_6$: C, 62.82; H, 4.74; N, 7.33. Found: C, 62.85; H, 4.72; N, 7.32.

4.1.4.15. 2-(3-Acetyl-5-(2,3-dihydrobenzo[b][1,4]dioxin-6-yl)-2,3-dihydro-1,3,4-oxadiazol-2-yl)-4-chlorophenyl acetate (5o). Light yellow, Yield 65%, mp: 192–193 °C. 1H NMR (300 MHz,

$DMSO-d_6$) δ : 2.12–2.17 (m, 6H), 4.30–4.31 (m, 4H), 7.00 (d, $J = 8.4$ Hz, 1H), 7.12 (s, 1H), 7.20–7.31 (m, 3H), 7.55–7.59 (m, 1H), 7.63 (s, 1H). MS (ESI): 417.8 ($C_{20}H_{18}ClN_2O_6$, $[M+H]^+$). Anal. Calcd for $C_{20}H_{17}ClN_2O_6$: C, 57.63; H, 4.11; N, 6.72. Found: C, 57.60; H, 4.12; N, 6.74.

4.1.4.16. 2-(3-Acetyl-5-(2,3-dihydrobenzo[b][1,4]dioxin-6-yl)-2,3-dihydro-1,3,4-oxadiazol-2-yl)-4-bromophenyl acetate (5p). Light yellow, Yield 67%, mp: 204–206 °C. 1H NMR (300 MHz, $DMSO-d_6$) δ : 2.11–2.17 (m, 6H), 4.28–4.31 (m, 4H), 7.01 (d, $J = 8.4$ Hz, 1H), 7.12 (s, 1H), 7.19–7.22 (m, 2H), 7.30 (dd, $J = 8.43$ Hz, 1H), 7.68–7.72 (m, 1H), 7.77 (d, $J = 2.4$ Hz, 1H). MS (ESI): 462.3 ($C_{20}H_{18}BrN_2O_6$, $[M+H]^+$). Anal. Calcd for $C_{20}H_{17}BrN_2O_6$: C, 52.08; H, 3.71; N, 6.07. Found: C, 52.04; H, 3.73; N, 6.06.

4.1.4.17. 2-(3-Acetyl-5-(2,3-dihydrobenzo[b][1,4]dioxin-6-yl)-2,3-dihydro-1,3,4-oxadiazol-2-yl)-4,6-dichlorophenyl acetate (5q). Brown solid, Yield 66%, mp: 156–157 °C. 1H NMR (300 MHz, $DMSO-d_6$) δ : 2.14–2.18 (m, 6H), 4.29–4.30 (m, 4H), 6.99 (d, $J = 8.6$ Hz, 1H), 7.14 (s, 1H), 7.19 (d, $J = 2.0$ Hz, 1H), 7.28 (dd, $J = 8.4$ Hz, 1H), 7.70 (d, $J = 2.6$ Hz, 1H), 7.91 (d, $J = 2.6$ Hz, 1H). MS (ESI): 452.3 ($C_{20}H_{17}Cl_2N_2O_6$, $[M+H]^+$). Anal. Calcd for $C_{20}H_{16}Cl_2N_2O_6$: C, 53.23; H, 3.57; N, 6.21. Found: C, 53.20; H, 3.58; N, 6.22.

4.1.4.18. 2-(3-Acetyl-5-(2,3-dihydrobenzo[b][1,4]dioxin-6-yl)-2,3-dihydro-1,3,4-oxadiazol-2-yl)-4,6-dibromophenyl acetate (5r). Light yellow solid, Yield 61%, mp: 177–178 °C. 1H NMR (300 MHz, $DMSO-d_6$) δ : 2.16–2.17 (m, 6H), 4.30–4.32 (m, 4H), 7.02 (d, $J = 8.4$ Hz, 1H), 7.14 (s, 1H), 7.21 (s, 1H), 7.30 (d, $J = 8.4$ Hz, 1H), 7.86 (d, $J = 2.2$ Hz, 1H), 8.13 (d, $J = 1.3$ Hz, 1H). MS (ESI): 540.2 ($C_{20}H_{17}Br_2N_2O_6$, $[M+H]^+$). Anal. Calcd for $C_{20}H_{16}Br_2N_2O_6$: C, 44.47; H, 2.99; N, 5.19. Found: C, 44.44; H, 2.98; N, 5.21.

4.1.4.19. 1-(5-(2,3-Dihydrobenzo[b][1,4]dioxin-6-yl)-2-(naphthalen-1-yl)-1,3,4-oxadiazol-3(2H)-yl)ethanone (5s). White crystal, Yield 66%, mp: 167–168 °C. 1H NMR (300 MHz, $CDCl_3$) δ : 2.45 (s, 3H), 4.24–4.27 (m, 4H), 6.84–6.91 (m, 1H), 7.35–7.38 (m, 2H), 7.44–7.63 (m, 4H), 7.75 (s, 1H), 7.90 (d, $J = 7.7$ Hz, 2H), 8.21 (d, $J = 8.6$ Hz, 1H). MS (ESI): 375.4 ($C_{22}H_{19}N_2O_4$, $[M+H]^+$). Anal. Calcd for $C_{22}H_{18}N_2O_4$: C, 70.58; H, 4.85; N, 7.48. Found: C, 70.56; H, 4.86; N, 7.46.

4.2. Cytotoxicity test

The cytotoxic activity *in vitro* was measured using the MTT assay. Cells were cultured in a 96-well plate at a density of 5×10^5 cells and different concentrations of compounds were respectively added to each well. The incubation was permitted at 37 °C, 5% CO_2 atmosphere for 24 h before the cytotoxicity assessments. 20 μ L MTT reagent (4 mg/mL) was added per well 4 h before the end of the incubation. Four hours later, the plate was centrifuged at 1200 rcf for 5 min and the supernatants were removed, each well was added with 200 μ L DMSO. The absorbance was measured at a wavelength of 570 nm (OD570 nm) on an ELISA microplate reader. Three replicate wells were used for each concentration and each assay was measured three times, after which the average of CC_{50} and SD were calculated. The cytotoxicity of each compound was expressed as the concentration of compound that reduced cell viability to 50% (CC_{50}). The results were summarized in Table 3.

4.3. Cell proliferation assay

Cells were activated by Con A (5 μ g/mL) for 24 h. Then, 5×10^5 cells were plated into 96-well plate per well with 5 μ g/mL Con A. After that, different concentrations of compounds were added to

each well, respectively. The cells were incubated for 72 h. 20 μ L MTT reagent (4 mg/mL) was added per well 4 h before the end of the incubation. Four hours later, the plate was centrifuged at 1200 rcf for 5 min and the supernatants were removed, each well was added with 200 μ L DMSO. The absorbance was read at a wavelength of 570 nm (OD570 nm) on an ELISA microplate reader. IC₅₀ was calculated and the results were summarized in Table 3. The immunosuppressive activity of each compound was expressed as the concentration of the compound that inhibited ConA stimulated T cell proliferation to 50% (IC₅₀) of the control value. The selective index (SI) value was used to evaluate the bioactivity of the compounds. The selective index (SI) is determined as the ratio of the concentration of the compound that reduced cell viability to 50% (CC₅₀) to the concentration needed to inhibit the proliferation to 50% (IC₅₀) of the control value.

4.4. PI3K γ inhibitory assay

Nineteen 1,3,4-oxadiazole derivatives containing 1,4-benzodioxan were tested in a search for small molecule inhibitors of PI3K γ , which was purchased from R&D Systems (Minneapolis, MN). PI3K γ was incubated for 4 h at room temperature with or without the presence of the oxadiazoles derivatives, the final concentration of drug as 3, 10, 30 and 50 μ M. The results were summarized in Table 4.

4.5. Cell apoptosis test

Lymph node cells were stimulated with Con A (5 μ g/mL) for 24 h. Then, 3×10^6 cells were plated into a 24-well plate per well, compounds of different concentrations were added to the plate and incubate with the cells for 24 h. The cells were harvested and stained with Annexin V-FITC for 20 min. The samples were analyzed by flow cytometer (FCM).

4.6. Western blotting

After incubation, cells were harvested and washed with PBS, then lysed in lysis buffer (30 mM Tris, pH 7.5, 150 mM NaCl, 1 mM phenylmethylsulfonyl fluoride, 1 mM Na₃VO₄, 1% Nonidet P-40, 10% glycerol, and phosphatase and protease inhibitors). After centrifugation at 12,000 g for 5 min, the supernatant was collected as total protein. The concentration of the protein was determined by a BCATM protein assay kit (Pierce, Rockford, IL, USA). The protein samples were separated by 10% SDS-PAGE and subsequently electrophoretically transferred onto a polyvinylidene difluoride membrane (Millipore, Bedford, MA, USA). The membrane was blocked with 5% nonfat milk for 2 h at room temperature. The blocked membrane was probed with the indicated primary antibodies overnight at 4 °C, and then incubated with a horse radish peroxidase (HRP)-coupled secondary antibody. Cleaved Caspase 3 and p-AKT (pS473) were measured as shown in Figure 4.

4.7. Molecular docking

The PI3K γ -LXX protein-ligand complex crystal structure (PDB ID: 3L54) was chosen as the template to compare the docking mode between compound **5q** bound to PI3K.³⁰ The molecular docking procedure was performed by using LigandFit protocol within Discovery Studio 3.1. For ligand preparation, the 3D structures of compound **5q** were generated and minimized using Discovery Studio 3.1. For enzyme preparation, the hydrogen atoms were added, and the water and impurities were removed. The whole PI3K enzyme was defined as a receptor and the site sphere was selected based on the ligand binding location of LXX, then the LXX molecule was removed and compound **5q** was placed during the molecular

docking procedure. Types of interactions of the docked enzyme with ligand were analyzed after end of molecular docking. Ten docking poses were saved for each ligand and the final docked conformation was scored.

4.8. Crystal structure determination

Crystal structure determination of compound **5q** were carried out on a Nonius CAD4 diffractometer equipped with graphite-monochromated Mo K α ($k = 0.71073$ Å) radiation (Fig. 2). The structure was solved by direct methods and refined on F^2 by full-matrix least-squares methods using SHELX-97.³¹ All non-hydrogen atoms of compound **5q** were refined with anisotropic thermal parameters. All hydrogen atoms were placed in geometrically idealized positions and constrained to ride on their parent atoms.

Acknowledgments

This work was financed by National Natural Science Foundation of China (No. J1103512).

References and notes

- Hackstein, H.; Thomson, A. W. *Nat. Rev. Immunol.* **2004**, *4*, 24.
- Kahan, B. D. *Nat. Rev. Immunol.* **2003**, *3*, 831.
- Dumont, F. J. *Curr. Opin. Investig. Drugs* **2001**, *2*, 357.
- Auger, K. R.; Serunian, L. A.; Soltoff, S. P.; Libby, P.; Cantley, L. C. *Cell* **1989**, *57*, 167.
- Engelman, J. A.; Luo, J.; Cantley, L. C. *Nat. Rev. Genet.* **2006**, *7*, 606.
- Rommel, C.; Camps, M.; Ji, H. *Nat. Rev. Immunol.* **2007**, *7*, 191.
- Camps, M.; Rückle, T.; Ji, H.; Ardisson, V.; Rintelen, F.; Shaw, J.; Ferrandi, C.; Chabert, C.; Gillieron, C.; Francon, B.; Martin, T.; Gretener, D.; Perrin, D.; Leroy, D.; Vitte, P. A.; Hirsch, E.; Wymann, M. P.; Cirillo, R.; Schwarz, M. K.; Rommel, C. *Nat. Med.* **2005**, *11*, 936.
- Marone, R.; Cmiljanovic, V.; Giese, B.; Wymann, M. P. *Biochim. Biophys. Acta* **2008**, *1784*, 159.
- Vazquez, M. T.; Rosell, G.; Pujol, M. D. *Il Farmaco* **1996**, *51*, 215.
- Vazquez, M. T.; Rosell, G.; Pujol, M. D. *Eur. J. Med. Chem.* **1997**, *32*, 529.
- Harrak, Y.; Rosell, G.; Daidone, G.; Plescia, S.; Schillaci, D.; Pujol, M. D. *Bioorg. Med. Chem.* **2007**, *15*, 4876.
- Xu, M. Z.; Lee, W. S.; Han, J. M.; Oh, H. W.; Park, D. S.; Tian, G. R.; Jeong, T. S.; Park, H. Y. *Bioorg. Med. Chem.* **2006**, *14*, 7826.
- Spinelli, O. A. *Ital. Soc. Chem.* **1999**, *3*, 301.
- Conti, P.; Dallanocce, C.; Amici, M. D.; Micheli, C. D.; Klotz, K. N. *Bioorg. Med. Chem.* **1998**, *6*, 401.
- Bae, E. A.; Han, M. J.; Lee, M.; Kim, D. H. *Biol. Pharm. Bull.* **2000**, *23*, 1122.
- Han, C. *Cancer Lett.* **1997**, *114*, 153.
- Hamiltonmiller, J. M. T. *Antimicrobial. Agents Chemother.* **1995**, *39*, 2375.
- Manjunatha, K.; Poojary, B.; Prajwal, L. L.; Fernandes, J.; Kumari, N. S. *Eur. J. Med. Chem.* **2010**, *45*, 5225.
- Kumar, H.; Javed, S. A.; Khan, S. A. *Eur. J. Med. Chem.* **2008**, *43*, 2688.
- Chandra, T.; Garg, N.; Lata, S.; Saxena, K. K. *Eur. J. Med. Chem.* **2010**, *45*, 1772.
- Kim, E. J.; Kwon, K. J.; Park, J.-Y.; Lee, S. H.; Moon, C.-H.; Baik, E. J. *Brain Res.* **2002**, *941*, 1.
- Wipf, P.; Fletcher, J. M.; Scarone, L. *Tetrahedron Lett.* **2005**, *46*, 5463.
- Razavi, H.; Powers, E. T.; Purkey, H. E.; Adamski-Werner, S. L.; Chiang, K. P.; Dendle, M. T. A.; Kelly, J. W. *Bioorg. Med. Chem. Lett.* **2005**, *15*, 1075.
- Lv, P. C.; Li, H. Q.; Xue, J. Y.; Shi, L.; Zhu, H. L. *Eur. J. Med. Chem.* **2009**, *44*, 908.
- Cao, P.; Ding, H.; Ge, H. M.; Zhu, H. L. *Chem. Biodivers.* **2007**, *4*, 881.
- Lauren, L.; Lyda, M. R.; Megan, L.; Ryan, D.; Hilary, M.; Sameer, C.; Balaji, B.; Erin, L. B.; April, L. R.; Susan, L. M.; Moses, L. J. *Med. Chem.* **2010**, *53*, 325.
- Elias, M.; Stefano, A.; Roberto, C.; Sara, V.; Maria, C. C.; Maria, L. S.; Rita, M.; Matilde, Y.; Giosu, C.; Laura, C.; Peter, M.; Simona, D. *J. Med. Chem.* **2011**, *54*, 6394.
- Sun, J.; Cao, N.; Zhang, X. M.; Yang, Y. S.; Zhang, Y. B.; Wang, X. M.; Zhu, H. L. *Bioorg. Med. Chem.* **2011**, *19*, 4895.
- Pomel, V.; Klicic, J.; Covini, D.; Church, D. D.; Shaw, J. P.; Roulin, K.; Burgat-Charvillon, F.; Valognes, D.; Camps, M.; Chabert, C.; Gillieron, C.; Francon, B.; Perrin, D.; Leroy, D.; Gretener, D.; Nichols, A.; Vitte, P. A.; Carboni, S.; Rommel, C.; Schwarz, M. K.; Rückle, T. *J. Med. Chem.* **2006**, *49*, 3857.
- Knight, S. D.; Adams, N. D.; Burgess, J. L.; Chaudhari, A. M.; Darcy, M. G.; Donatelli, C. A.; Luengo, J. I.; Newlander, K. A.; Parrish, C. A.; Ridgers, L. H.; Sarpong, M. A.; Schmidt, S. J.; Van Aller, G. S.; Carson, J. D.; Diamond, M. A.; Elkins, P. A.; Gardiner, C. M.; Garver, E.; Gilbert, S. A.; Gontarek, R. R.; Jackson, J. R.; Kershner, K. L.; Luo, L.; Raha, K.; Sherik, C. S.; Sung, C.-M.; Sutton, D.; Tummimo, P. J.; Wegrzyn, R. J.; Auger, K. R.; Dhanak, D. *ACS Med. Chem. Lett.* **2010**, *1*, 39.
- Sheldrick, G. M. *SHELX-97. Program for X-ray Crystal Structure Solution and Refinement*; Göttingen University: Germany, 1997.